sciendo

Civil and Environmental Engineering
Vol. 18, Issue 1, 76-86, DOI: 10.2478/cee-2022-0008

NONLINEAR ANALYSIS OF HOLLOW SLENDER REINFORCED CONCRETE COLUMNS SUBJECTED TO CONCENTRIC AND ECCENTRIC LOADS

Wameedh Issa BRAIDI[1,*], Mohammed Salih Abd ALI[2]

[1] Department of Civil Engineering, University of Maisan, Iraq.
[2] Department of Civil Engineering, Southern Technical University, Amarah Technical Institute, Iraq.
[*] corresponding author: wameedhissa@uomisan.edu.iq

Abstract

This paper investigates the load capacity and failure modes of slender hollow RC column under axial and eccentric loads. For the slender hollow columns, different load eccentricities and hole shapes are used. The finite element software ABAQUS is used to model and analyze the columns. The experimental test result is used to conduct a verification investigation of the nonlinear finite element modeling. All specifications of the experimentally tested columns are taken into consideration in the modeling to establish the verification of the model. When the modeling and test results are compared, it is noticeable that they are in good agreement. As a result, the modeling's accuracy is proved. Then, a parametric study included different slenderness ratio, section shape, concrete strength and SFR strengthened has been done with the same modeling method. The effects of these variables on the column load capacity are investigated. It is found that increasing slenderness ratio led to smaller peak load. Increasing of moment of inertia of square and circular section decreased the peak load capacity. The maximum bearing capacity increased with higher concrete strength. Also, SFR distribution through the length of columns effected on load bearing capacity.

Keywords:

Hollow slender RC column;
Eccentricity;
Nonlinear analysis;
FE analysis;
Abaqus.

1 Introduction

In modern structural constructions, slender hollow RC columns are frequently used as dominating compression members. As a result, study into their load capacity and failure modes is necessary [1]. To minimize the cost of the constructions and to lessen their self-weight where it is necessary, hollow columns have been recommended over solid columns [2, 3]. In reinforced concrete columns, transverse openings and longitudinal holes are frequently included to give access for utilities like as plumbing and electrical wiring. ABAQUS is the most powerful software for this purpose, concrete damage plasticity model used in the simulation prosses shows the real behavior of concrete material that's lead to a good agreement between experimental and FE results [4, 5]. The previous studies on slender reinforced concrete columns using FE method can be citation as follows:

Nessa [6], complete a nonlinear finite element analysis for an axial loaded reinforced concrete column subjected to biaxial bending that took into account second-order effects. Second-order effects can be taken into account in two ways, according to Eurocode: nonlinear FE analysis and manual calculations based on Eurocode 2 simplified techniques. The bearing capacity from FE analysis was 21-34 percent higher than the one produced with the simplified methods, according to a comparison of results from the simplified method and ABAQUS, estimated with design parameters. Pragna and Ganesan [7], Examine the load-bearing capacity of concrete-filled steel tubes (CFT) subjected to compression loading. The study of CFT behavior and the different parameters that influence it is done with commercially available FEM software (ANSYS). Variable parameters such as the grade of concrete infill and the diameter to thickness ratio of the steel tube are used in a nonlinear finite element analysis of concrete filled steel tube. Raju et al. [8], studied the buckling behavior of an

imperfect columns and frames by considering a member whose axis is first bent and subjected to axial and lateral loads. The impact of flaws in the design of long and short columns and frames is investigated. ANSYS software is used to do analysis with and without imperfections. In columns and frames, the imperfection value is calculated and induced. Qiu et al. [9] used ABAQUS to create a numerical model that simulates the behavior of elliptical concrete-filled columns under concentric or eccentric compressive loads. The computational results for ultimate load, load–deflection behavior, and failure mechanisms were compared to a variety of experimental results, with good agreement found. Ihsan et al. [10], investigate the behavior of slender RC columns with longitudinal opening subjected axial compression load and uniaxial bending. The specimens of the research include the analysis of eight slender columns of dimensions 150 x 150 x 1300 mm. To simulate the behavior of reinforced concrete slender columns with longitudinal holes, a nonlinear finite element analysis was performed using the ANSYS. Two parameters are considered (longitudinal steel ratio of the column and grade of steel (*fy*)). The results reveal that increasing the steel ratio in hollow reinforced concrete slender columns increases the ultimate load by a substantial amount. Also, the increased steel ratio resulted in lower tensile steel stresses, particularly at the slender column's tension face, resulting in increased load carrying capability. Yonas et al. [11], discusses the behavior of slender concrete filled steel tube column subjected to eccentric loading using finite element analysis. Finite element package ABAQUS 6.13-1 is used to analyze the load carrying capacity of the composite columns. A general non-linear procedure is adopted for the prediction of mid height deflection and axial load carrying capacity with varying eccentricity. The result shows composite column with smaller eccentricity, large cross-sectional area and large thickness of steel tube can carry higher maximum load. Due to the increment of eccentricity from 0 mm to 157 mm the load carrying capacity decreases from 0 % to 32.71 %. Ihsan et al. [12], investigate the behavior of reinforced concrete slender columns with longitudinal hole under axial compression load and uniaxial bending. The study comprises the testing of ten thin columns with different dimensions 150 x 150 x 1300 mm. The research analyzes the impact of different column hole diameters. The influence of opening ratio on load capacity is minor when the openings are situated in the center of the column section and the column is loaded with high load eccentricity, according to test results. Lotfy [13], investigate the behavior of slender reinforced concrete columns subjected to eccentric loads strengthened with CFRPs in three different manners in order to improve its axial and flexural rigidity. Ten full-scale specimens with rectangular cross sections 210 mm x 150 mm were subjected to eccentric compressive force until they failed. Safaa and Alaa [14], using nonlinear finite element analysis, demonstrate the structural performance of slender SSRC columns using experimental and numerical methods. The research is based on nine RC specimens that were tested to failure, also eighteen FE models that were examined using the Abaqus soft wear program. When compared to equivalent square-shaped columns, the usage of SSRC columns increased strength by around 12 % and reduced deformations by nearly 40 %. The compressive strength of SSRC columns subjected to concentric loading has been calculated using two design formulas. When SSRC columns are compared to equivalent square-shaped columns, the results show that they perform well structurally. The subsistence of longitudinal holes in slender RC columns has been addressed to a limited number of numerical investigations. The purpose of this research was to investigate numerically hollow slender RC columns subjected to axial and eccentric loads. Also, a parametric study had been presented in this paper.

2 Methodology

This research is based on the verification of concrete columns casted and tested in Amarah Technical Institute laboratory by Alla Mohammed Sahi and Mohammed Salih Abd Ali (Experimental Study of Hollow Slender Reinforced Concrete Columns Subjected to Eccentric Loads). There were fifteen columns in total [2], five columns were selected to simulate using finite element method, first one concentrically loaded and the other four columns were designed with a corbel at the ends for testing under eccentric load as shown in Fig. 1. The different parameters that define the characteristics of the columns are shown in Table 1.

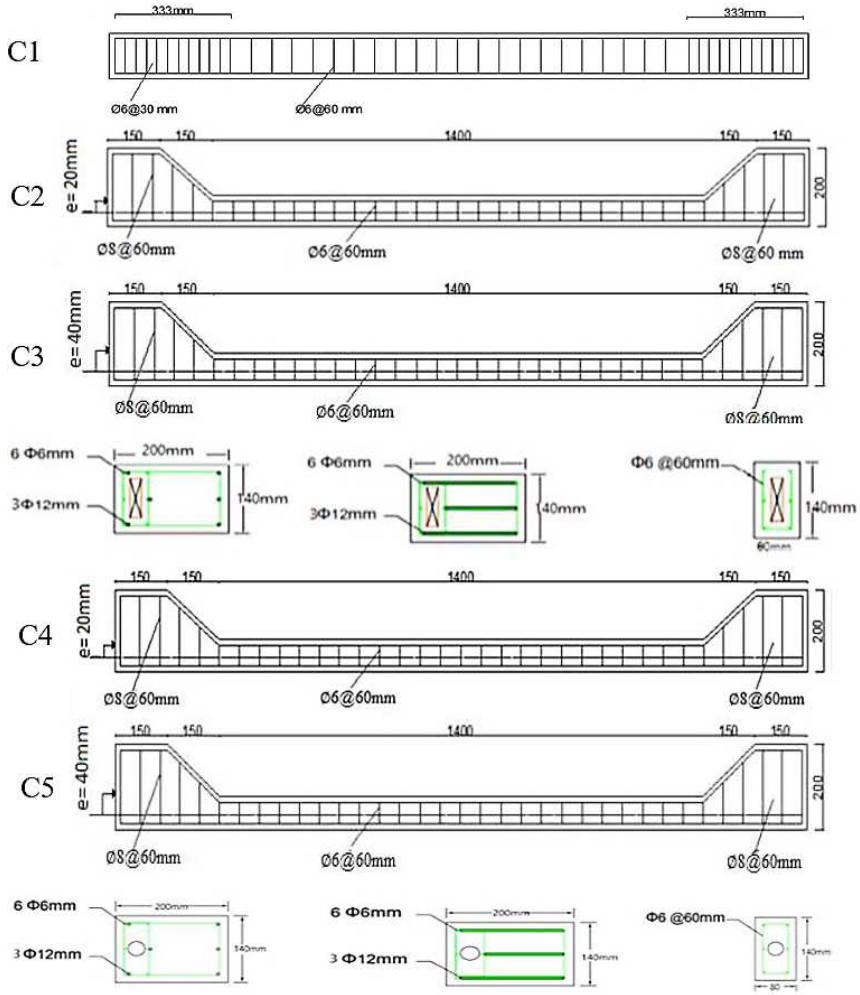

Fig. 1: Columns details by Alaa [2].

Table 1: Properties of tested columns.

Column ID	Dimension [mm]	Shape of opening	Dimension of opening [mm]	Eccentricity [mm]	Compressive strength $f_{c'}$ [N/mm^2]	Ultimate load test result [kN]
C1	80 x 140 x 2000	Rectangular	20 x 80	0	35	290
C2	80 x 140 x 2000	Rectangular	20 x 80	20	35	175
C3	80 x 140 x 2000	Rectangular	20 x 80	40	35	160
C4	80 x 140 x 2000	Circular	Ø 45	20	35	200
C5	80 x 140 x 2000	Circular	Ø 45	40	35	190

The compressive strength test of normal concrete f_{cu} was done by using six cubical specimens with dimension 150 x 150 x 150 mm at 28 days according to the British standard [15], ABAQUS requires concrete compressive strength input data for cylinder test $f_{c'}$.

2.1 Material models for nonlinear analysis

2.1.1 Concrete model

Concrete damaged plasticity (CDP) is a popular concrete model used in FEM analysis since it is primarily intended for reinforced concrete structures. Two main failure mechanisms of the CDP model are tensile cracking and compressive crushing of the concrete. Under low confining pressures and uniaxial compression and tension, concrete behaves brittle. When the confining pressure is high enough to prevent fracture propagation, this behavior changes, and when multiaxial compressive stresses are applied to concrete as shown in Fig. 2. The material becomes more ductile as a result, and its compressive strength rises.

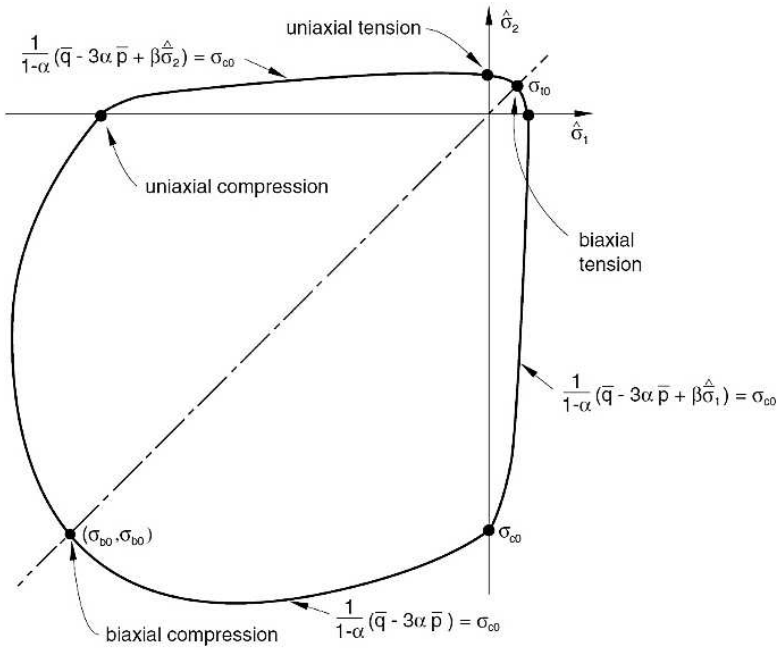

Fig. 2: Biaxial yield surface of concrete in CDP model (ABAQUS materials manual) [16].

Under compound stress, the default ABAQUS parameters of the concrete damage plasticity model are listed in Table 2.

Table 2: Default concrete damage plasticity parameters.

Ψ	e	f_{b0}/f_{c0}	k	μ
36°	0.1	1.16	0.667	0

Ψ - dilation angle, e - plastic potential eccentricity (shows the rate at which the function approaches asymptote in the hyperbolic surface of plastic potential in meridional plane in the stress-strain relation), f_{b0}/f_{c0} - the ratio of strength in the biaxial state to the strength in the uniaxial state, k - stress invariant ratio, μ - viscosity parameter.

2.1.2 Steel model

When taken as a whole, the stress-strain curve for steel is quite complicated. However, in most circumstances, an idealization that is typically utilized is elastic-perfectly plastic (non-strain hardening) [17]. The reinforcing steel bars were modeled using Abaqus' plasticity model, a bilinear model characterized the stress–strain relationship of reinforcement (elastic perfectly plastic) as shown in Fig. 3. The elastic modulus and Poisson ratio were set to 200 GPa, and 0.3 respectively, since the steel elasto-plastic model were used ABAQUS requires initial yield stress at zero plastic strain, therefore yield strength and plastic strain were set to 410 MPa and 0 respectively [18].

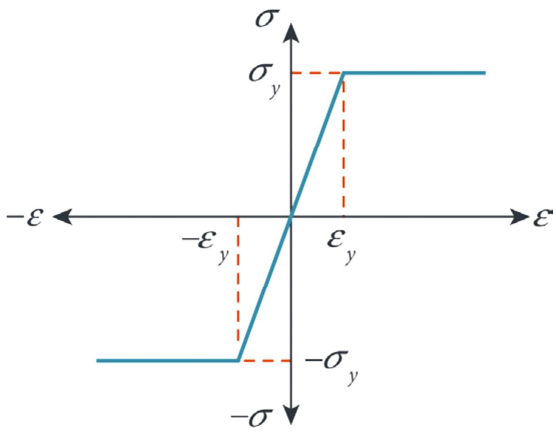

Fig. 3: Idealized elasto-plastic stress-strain curve for steel by Anwar [17].

2.2 Modelling

A precise model of the structural elements and constituent members working as a composite made up of concrete and steel is required for numerical simulation of a reinforced concrete structure. ABAQUS is used to create a distinct sketch for each segment. Fig. 4 shows all model sections.

One of the most powerful special constraint features in ABAQUS is the embedded region constraint, which used to merge the reinforcement bars with the concrete as shown in Fig. 5.

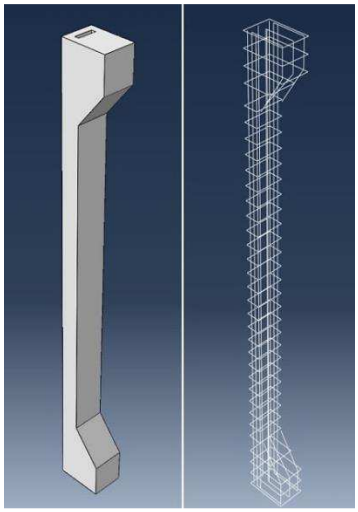

Fig. 4: Concrete and steel sections.

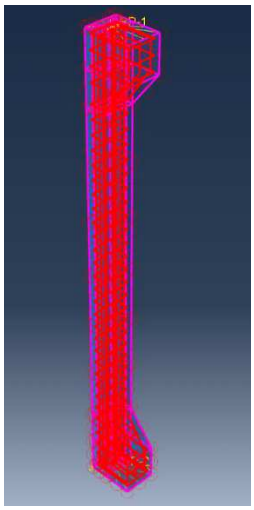

Fig. 5: Embedded region constraint.

2.2.1 Meshing

A rectangular mesh was utilized to produce good results from the model. The mesh elements were 20 mm in size. A mesh size of 10 mm might have been chosen, but that would have resulted in a lot more elements and more computational time with similar results. Table 3 shows mesh details for each of the column's components.

Table 3: Meshing details.

Part	Type of element	Material type
Concrete column	C3D8 (8-node linear brick)	Concrete
Reinforcement	T3D2 (2-node linear 3-D truss)	Steel

The reinforcement nodes line up with the concrete column's nodes. This increases the model's accuracy and, as a result, the quality of the outputs as shown in Fig. 6.

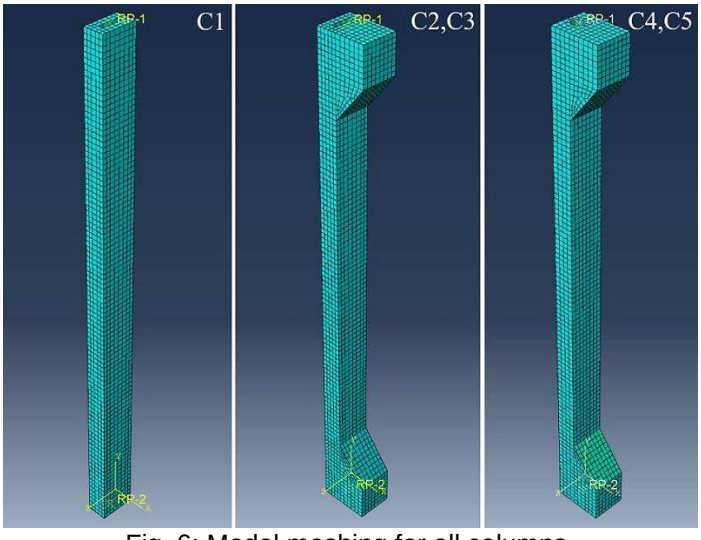

Fig. 6: Model meshing for all columns.

2.2.2 Boundary conditions and loads

The support conditions were modelled as pin-pin end conditions to simulate the experimental columns. In order to imitate these conditions, reference point at the lower end of the column was selected with restraining the *x*, *y* and *z*-axis movement of this point as in Fig. 7. Similarly, the upper pin end conditions were defined, only the displacement towards the *x* and *z*-axis were restrained. The load was applied as a displacement through *y*-axis, as shown in Fig. 8.

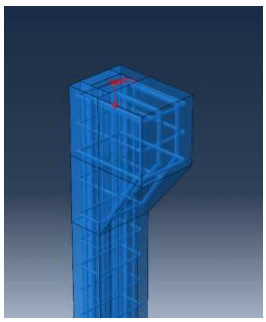

Fig. 7: Pinned support conditions.

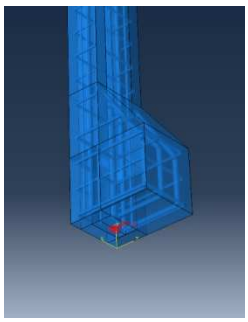

Fig. 8: Load and support conditions.

3 Results and discussions

3.1 Failure mode

The inception of cracks is seen at the mid-height of the column as the load increased until failure. Fig. 9 shows the failure mode in the slender RC columns that have been analyzed and which also gave good compatibility with the experimental models.

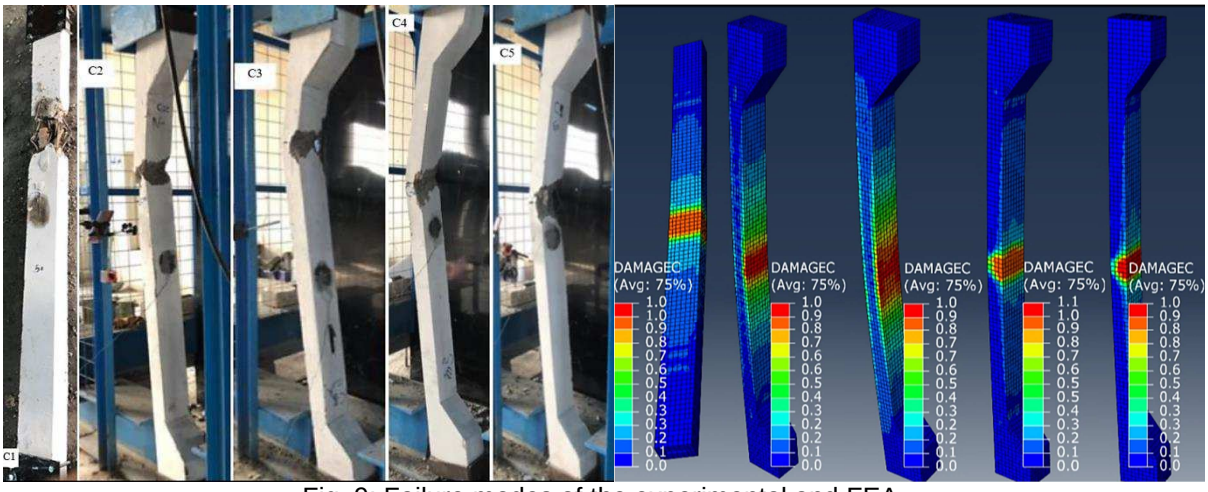

Fig. 9: Failure modes of the experimental and FEA.

3.2 Ultimate failure point

The comparison of ultimate load and maximum deflection between finite element and experimental results are shown in Table 4. This indicates that the agreement between finite element results and experimental results are excellent.

Table 4: Results of the experimental test and finite element analysis.

Column ID	$P_{Exp.}$ [kN]	P_{FEA} [kN]	$P_{FEA}/P_{Exp.}$
C1	290	291.69	1.00
C2	175	170.7	0.97
C3	160	150.92	0.94
C4	200	181.13	0.90
C5	190	171.39	0.90

P_{Exp} - maximum load achieved in experiments, P_{FEA} - maximum load achieved in the numerical model.

3.3 Load-deflection response

Dial gage of an accuracy of 0.01 mm were placed on the surface of the column mid-height to measure the lateral displacement, all columns experimental results recorded. The load-deflection curves obtained from FE were compared to those obtained from test data as shown in Fig. 10. In the start of the numerical model load- deflection curve records zero deformations up to about 40, 50 kN resulting from the imperfection conditions, ABAQUS assumed perfect material and perfect boundary conditions for any model, but in reality, there are no perfect material structure especially concrete and no perfect column ends fixation conditions. For the rising part of the load-deflection curves, the curves exhibit adequate convergence between test and numerical results.

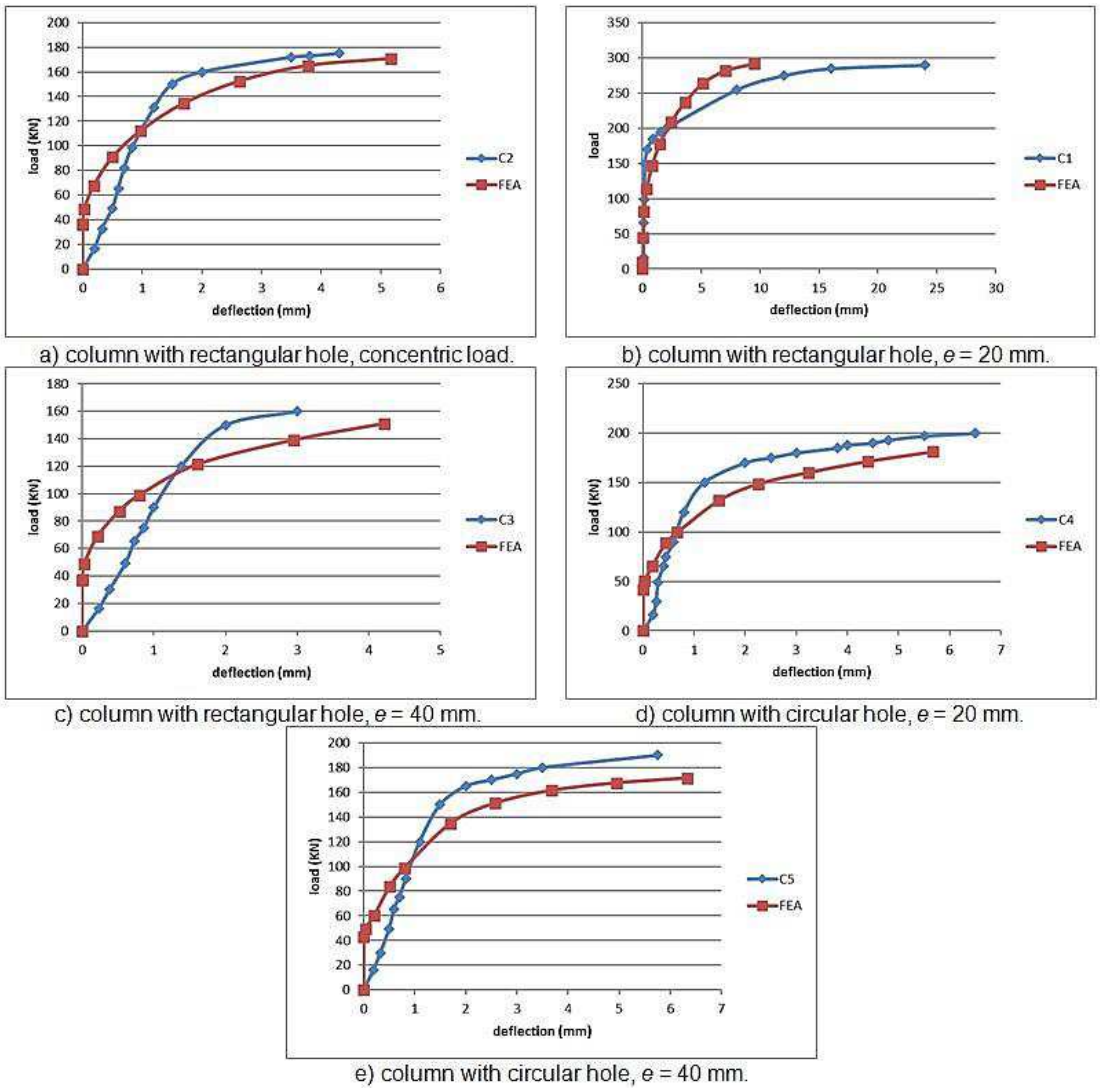

a) column with rectangular hole, concentric load.
b) column with rectangular hole, e = 20 mm.
c) column with rectangular hole, e = 40 mm.
d) column with circular hole, e = 20 mm.
e) column with circular hole, e = 40 mm.

Fig. 10: Load displacement curve for FEA and experimental results.

4 Parametric studies

The major objective of the present paper is to study the effect of two parameters, load eccentricity and opening shape. Laboratory tests provide results without covering a large number of variables since it necessitates the use of expensive equipment and tools, as well as a specialized laboratory with qualified staff to complete the experiments and the finite element technique FEM is the most appropriate tool for expanding the range of parameters to be explored. A three-dimensional nonlinear numerical analysis has been carried out to simulate the imperfection scale factor effect on RC columns buckling using the ABAQUS/Standard 2020 software. Slenderness ratio, section shape, concrete strength, strengthening with SFR are the parameters that were taken into account in this research, the FE model C1 was used as a reference as shown in Table 5 and Fig. 11.

Table 5: Results of the parametric study.

ID	Section shape	Section dimension [mm]	Length	Slenderness ratio	Shape of opening	Opening dimension [mm]	Eccentricity [mm]	Compressive strength $f_{c'}$ [N/mm^2]	SFR distribution	Ultimate load [kN]	U_p/U_{C1}
C1	Rectangular	80 x 140	2000	80.5	Rectangular	20 x 80	0	35	-	291.69	-
H1	Rectangular	80 x 140	1500	60.4	Rectangular	20 x 80	0	35	-	316.99	1.09
H2	Rectangular	80 x 140	2500	100.7	Rectangular	20 x 80	0	35	-	273.75	0.94
H3	Rectangular	80 x 140	3000	120.8	Rectangular	20 x 80	0	35	-	261.86	0.90
H4	Square	106 x 106*	2000	80.5	Square	40 x 40*	0	35	-	327.48	1.12
H5	Circular	Ø 119.4*	2000	80.5	Circular	Ø 45*	0	35	-	326.66	1.12
H6	Elliptical	*a,b* = 80,44.5*	2000	80.5	Elliptical	*a,b* = 40,13*	0	35	-	290.53	1
H7	Rectangular	80 x 140	2000	80.5	Rectangular	20 x 80	0	25	-	231.98	0.79
H8	Rectangular	80 x 140	2000	80.5	Rectangular	20 x 80	0	40	-	320.05	1.9
H9	Rectangular	80 x 140	2000	80.5	Rectangular	20 x 80	0	45	-	349.4	1.2
H10	Rectangular	80 x 140	2000	80.5	Rectangular	20 x 80	0	35	L	349	1.2
H11	Rectangular	80 x 140	2000	80.5	Rectangular	20 x 80	0	35	L/2	388.68	1.33
H12	Rectangular	80 x 140	2000	80.5	Rectangular	20 x 80	0	35	L/3	277.23	0.95

* These dimensions give the equivalent rectangular section or opening area where U_p/U_{C1} - FE parametric column ultimate load / FE C1 ultimate load , SFR distribution columns H10, H11, and H12 were strengthened by steel fibers all the column, 50 % of the column length in the middle, and 33.3 % of the column length in the middle respectively [19].

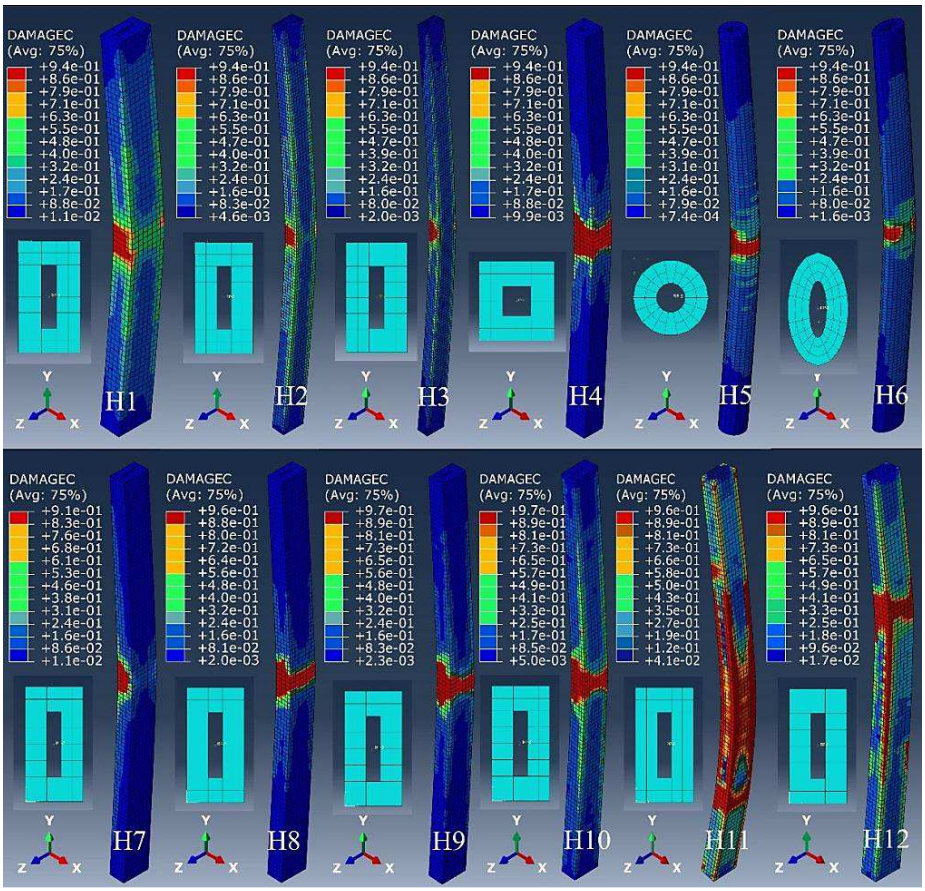

Fig. 11: ABAQUS parametric study results.

4.1 Slenderness ratio

Column H1 was shorter 1.5 m and slender less than column C1, columns H2 and H3 were longer and slenderer than column C1. As can be observed, slenderness results in a lower peak load, Fig. 12.

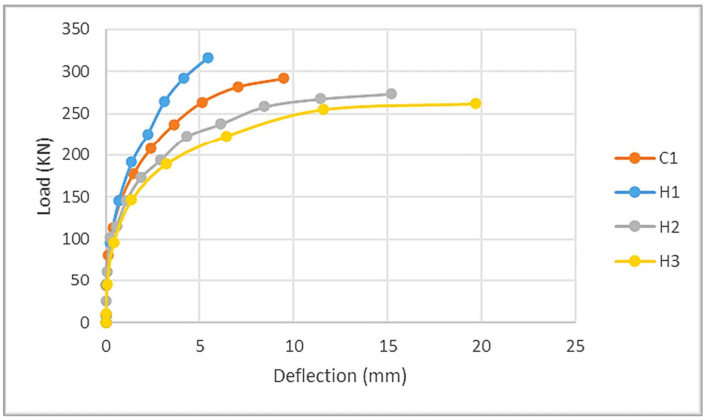

Fig. 12: Slenderness ratio parameters.

4.2 Section shape

The peak load obtained from column H6 were the same as reference column C1 resulting from the similarity of moment of inertia for both rectangular and elliptical section with equivalent section area, but as seen in columns H4 and H5 the change in section dimensions values leads to increase in moment of inertia for each column section, as a result stiffness increased, that lead to increase of peak load of 12 %, Fig. 13.

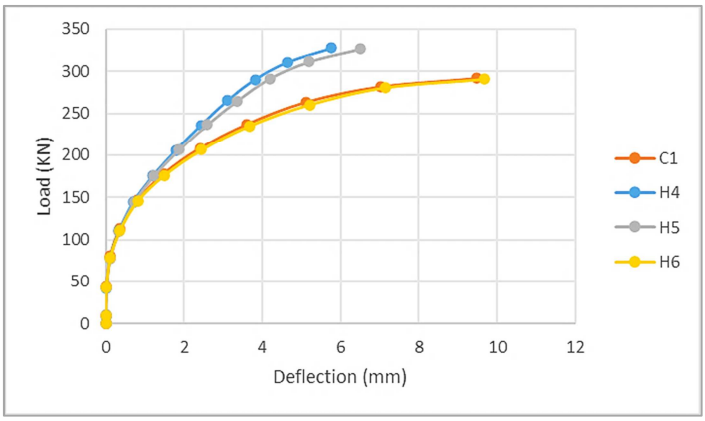

Fig. 13: Section shape parameters.

4.3 Concrete strength

Column H7 had lower strength 25 MPa than column C1, column H8 and H9 had higher strength 40 MPa and 45 MPa than column C1. Although the buckling in slender columns depends on geometry, it can be seen that the compressive strength will affect; therefore, with increased concrete strength, the maximum bearing capacity increases, Fig. 14.

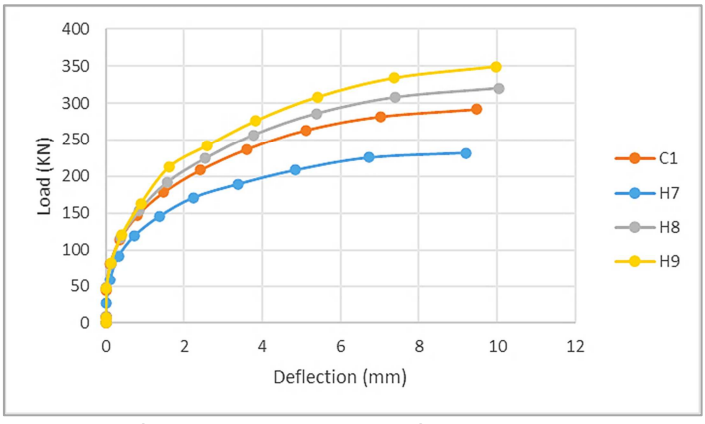

Fig. 14: Concrete strength parameters.

4.4 Strengthening with SFR

Column H10, H11 and H12 the SFR distribution through the length of columns lead to increase in bearing capacity 20 % for column H10 and 33 % for column H11 and decreased in bearing capacity 5 % for column H12, Fig. 15.

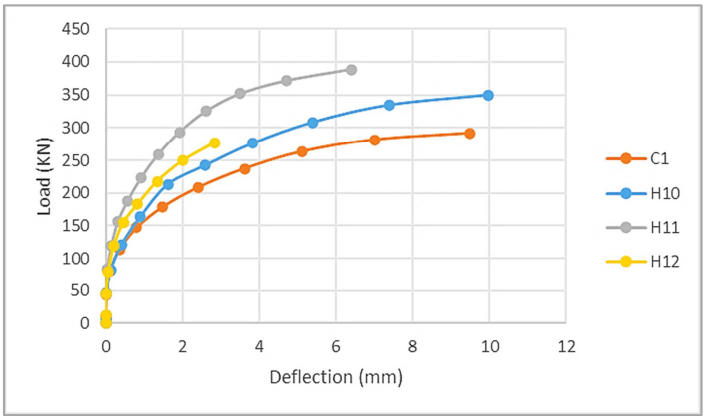

Fig. 15: SFR strengthening parameters.

5 Conclusions

In this study, 3D reinforced concrete hollow columns were analyzed in ABAQUS. These models took into account the concentric and eccentric loads and hole shape parameters, and was confirm by making a comparison between the FE results and the experimental study results. The following conclusions were drawn based on the experimental tests and FE results:

1) Concrete showed a perfectly nonlinear behavior in both experimental and FE results.

2) Agreement between experimental and FE results proved that the finite element software is effective enough.

3) For columns that have different slenderness ratio H1, H2 and H3, comparing the results with reference column C1, it is found that the ultimate load of column H1 increased by 9 %, while the ultimate load of columns H2 and H3 decreased by 6 % and 10 % respectively, the increase in slenderness ratio decreases the column ultimate load.

4) Column section geometry will have an effect, square and circular columns have a greater buckling resistance by 12 % than rectangular and elliptical columns with the same cross-sectional area, square and circular columns showed a stiffer behavior than the others.

5) Although in slender columns buckling is controlled by geometry more than material strength, there was an effect of the material compressive strength variation with the same slenderness ratio, it is found that columns that have a greater compressive strength, have a higher ultimate load.

6) Also, strengthened concrete by steel fiber reinforcement by different ratios, will affect in ultimate load, column H10 and H11 showed higher ultimate load by 20 % and 33 % respectively compared to column C1, while column H12 ultimate load were less than column C1 by 5 %, column H12 buckle in the point where normal concrete met the strengthened concrete not at its mid height, which make the decrease in ultimate load acceptable, although the column was strengthened by SFR compared to column C1.

References

[1] BAHRAMI, A. – KOUHI, A. M.: Load Capacity and Failure Modes of Axially and Eccentrically Loaded Thin-Walled Steel Tubular Slender Columns Filled with Concrete. International Journal on Emerging Technologies, Vol. 11, Iss. 5, 2020, pp. 517-524.

[2] SAHI, A. M. – ALI, M. S. A.: Experimental Study of Hollow Slender Reinforced Concrete Columns Subjected to Eccentric Loads. Civil and Environmental Engineering, Vol. 17, Iss. 1, 2021, pp. 303-317.

[3] AL-HELFI, M. – ALLAMI, A.: Experimental Work to Study the Strengthening Effect of SFR and CFRP on Part or Whole Length of Slender RC Columns. Civil and Environmental Engineering, Vol. 17, Iss. 1, 2021, pp. 9-22.

[4] DASSAULT SYSTEMS.: ABAQUS Analysis Manual 4.14, 2014.

[5] BARBERO, E. J.: Finite Element Analysis of Composite Materials Using Abaqus. Taylor & Francis Group, LLC, 2013.
[6] ARYA, N. Y. N.: Second-order FE Analysis of Axial Loaded Concrete Members According to Eurocode 2. Royal Institute of Technology (KTH), Department of Civil and Architectural Engineering, Stockholm, Sweden, 2015, Master Thesis 466.
[7] PRAGNA, M. – GANESAN, P.: Analysis of Concrete Filled Steel Tubes using Ansys. International Journal of Latest Engineering Research and Applications (IJLERA), Vol. 1, Iss. 9, 2016, pp. 71-78.
[8] RAJU, J. N. S. S. – RAO, M. V. – SABARISH, G. – RAO, P. V.: Effect of Imperfections on Stability of Column and Frame. International Journal of Engineering Research & Technology (IJERT), Vol. 5, Iss. 11, 2016.
[9] QIU, W. – MCCANN, F – ESPINOS, A. – ROMERO, M. L. – GARDNER, L.: Numerical analysis and design of slender concrete-filled elliptical hollow section columns and beam-columns. Engineering Structures, Vol. 131, 2017, pp. 90-100.
[10] AL-SHAARBAF, I. A. S. – HAMOOD, M. J. – AL-ZAIDY, E. A. A.: Nonlinear analysis of hollow slender reinforced concrete columns under eccentric loading. University of Thi-Qar Journal, Vol. 13, Iss. 4, 2018.
[11] YONAS, T. Y. – TEMESGEN, W. – SENSHAW, F. W.: Finite Element Analysis of Slender Composite Column Subjected to Eccentric Loading. International Journal of Applied Engineering Research, Vol. 13, Iss. 15, 2018, pp. 11730-11737.
[12] AL-SHAARBAF, I. A. S. – AL-ZUBAIDI, M. J. H. – AL-ZAIDY, E. A. A.: Effect of Hollowing Ratio on the Behavior of Hollow Self-Compacting Reinforced Concrete Slender Column under Eccentric Loading. International Journal of Engineering & Technology, Vol. 7, Iss. 4.20, 2018, pp. 390-394.
[13] LOTFY, E. M.: Numerical Study of Long Columns Strengthened by Fiber Reinforced Polymer (FRP). International Journal of Engineering Science & Research Technology, Vol. 7, Iss. 5, 2018.
[14] ABDUALRAHMAN, S. Q. – AL-ZUHAIRI, A. H.: A Comparative Study of the Performance of Slender Reinforced Concrete Columns with Different Cross-Sectional Shapes. MDPI, fibers, Vol. 8, Iss. 35, 2020.
[15] BS 8110: Part 1 & 2: Structural use of concrete, British Standard – British Standard Institution, 1985.
[16] DASSAULT SYSTEMS.: ABAQUS Materials Manual 4.14, 2014.
[17] ANWAR, N. – NAJAM, F. A.: Structural Cross-Sections Analysis and Design. Butterworth-Heinemann, Elsevier, 2017.
[18] DASSAULT SYSTEMS.: Getting started with Abaqus 4.14, 2014.
[19] ALI, M. S. A. – ALLAMI, A.: Experimental Work to Study the Strengthening Effect of SFR and CFRP on a Part or Whole of the Length of Slender RC Columns. Civil and Environmental Engineering, Vol. 17, Iss. 1, 2021, pp. 9-22.